JOURNAL OF MATERIALS SCIENCE 39 (2004) 7193–7197

# Multiscale modelling of microstructure formation during vacuum arc remelting of titanium 6-4

R. C. ATWOOD, P. D. LEE
*Department of Materials, Imperial College London, SW7 2BP, UK*
*E-mail: r.atwood@imperial.ac.uk*

R. S. MINISANDRAM, R. M. FORBES JONES
*ATI Allvac, Monroe, North Carolina, USA*

The vacuum arc remelting of titanium 6-4 alloy is a complex process. Relatively high melt currents ($\geq$30 kA) are used resulting in a very deep melt pool that is continually changing in size (first increasing and then decreasing). The process is further complicated due to the use of external stirring coils to control and steer the arc. A transient model is needed to adequately describe the process. A multiscale modelling approach was developed which combines an axisymmetric CFD model at the macroscale with a cellular automaton model at the mesoscale. The macro model is used to simulate the heat and mass transfer throughout the ingot and melt pool under the influence of the arc, including EMF. A decentred-square cellular automaton model is used to predict the nucleation and growth of grains. This multiscale model is applied to the initial phase of the process, and the predicted microstructures are compared with trial ingots. The effect of the model parameters such as stirring and grain nucleation on the morphology of the columnar zone is investigated. © *2004 Kluwer Academic Publishers*

## 1. Introduction

The Vacuum Arc Remelting (VAR) process is used as secondary processing for the homogenization of high-melting-point and oxygen-sensitive materials such as superalloys and titanium alloys. For Ti alloys, it is common to reduce electrode-crucible arc-shorts through the use of axial magnetic induction provided by an external coil concentrically wound around the crucible. This magnetic steering of the arc also has the effect of stirring the liquid metal, and is often referred to as the 'stirring field'.

Previous simulations [1] have suggested that the magnetic field within the ingot becomes progressively reduced during the VAR process, providing an explanation of the observed distribution of columnar and equiaxed areas of the ingot. However, the previous studies have not considered the effect of the development of microstructure or the effect of the nucleation behaviour on the columnar/equiaxed transition. In this paper a microstructural model coupled to the VAR simulation is used to investigate how the parameters which affect nucleation affects this transition.

## 2. Methods

### 2.1. Experimental

A Ti-6Al-4V electrode of diameter 0.762 m was remelted in a production furnace into an ingot 0.864 m in diameter. Other production details, including melt schedule have been previously presented [1]. The ingot was sectioned, polished and etched using standard $HNO_3$/HF etchant in order to bring out the grain macrostructure that was presented in its entirety [1].

### 2.2. Modelling theory

A multiscale approach was used, applying a model with a node spacing of order 10 mm to solve the heat transfer, electromagnetic effects, and fluid flow (the macromodel) and a model with a node spacing of order 800 $\mu$m to simulate the grain formation (the mesomodel).

#### *2.2.1. Multiscale link*

The temperature used by the mesomodel was obtained from the macromodel by using bi-linear interpolation from the temperature at the macromodel nodes, followed by linear interpolation between the macromodel output steps. The output steps were spaced at 120 s intervals. Any part of the domain located above the macro mesh was assigned the maximum temperature found in the macro mesh, and any part located below the macro mesh was assigned the minimum. This was necessary because the macro mesh stretches as the mould is filled whereas the CA domain is static. Unfortunately this resulted in some irreducible sharp changes in the temperature profile, which affected the simulated microstructure in some cases.

### 2.2.2. Macroscale

An axisymmetric finite-difference based VAR model developed by the Specialty Metals Processing Consortium (SMPC), BAR-v453, was used to simulate the arc melting process. In addition to the standard equations for heat transfer, fluid flow and electromagnetic effects due to the melt current, the model incorporates a 2-½-D approximation for flow in order to capture the effect of external stirring [1–3]. The applied field was 60 G with a reversal time of 40 s.

TABLE I Simulation parameters

| Property | Value | Unit |
|---|---|---|
| Average nucleation undercooling | 1–32 | K |
| Nucleation undercooling Std. deviation | 0.5–8 | K |
| Total volume density of nuclei | $5 \times 10^7$–$5 \times 10^8$ | $1/m^3$ |
| Growth coefficient | 5.85e-6 | m/s/K |
| Grid | $740 \times 540$ | – |
| Cell size | 800 $\mu$m | m |
| Time step | 1 | s |

### 2.2.3. Mesoscale

The development of the microstructure was modelled in response to the change in temperature predicted by the macromodel. The method used an approach similar to the model presented by Gandin and Rappaz [5] with modifications to the decentred square method used by Wang *et al*. [6]. In brief, the domain is divided into a regular array of square cells, significantly smaller than the macromodel elements. If a cell contains some solid, the solid grows at a rate $v$ determined by the undercooling $\Delta T$ and growth coefficient $\alpha_g$,

$$v = \alpha_g \Delta T^2. \quad (1)$$

The growth rate determines the positions of the corners of a square within each cell, whose orientation and centre offset with respect to the cell represent the crystallographic orientation and preferred growth direction of the grain. This allows a population of grains to be simulated, each grain having its own preferred growth direction and thus improves on the previously presented model for VAR microstructure prediction [7]. The decentred-square mesomodel of Wang *et al*., which is discussed in greater detail elsewhere [6] is used.

The initiation of grains is simulated by a stochastic nucleation process, in which a random selection of nuclei, each having its own critical undercooling, is distributed throughout the domain, as described by Atwood and Lee [8]. The number of nuclei, $N_n^{\Delta T}$, was taken as a Gaussian function of undercooling, characterized by three parameters: the total number density of nuclei, $N_n^v$; the average undercooling, $\Delta T_n$; and the standard deviation, $\sigma_n$. In addition, pre-existing

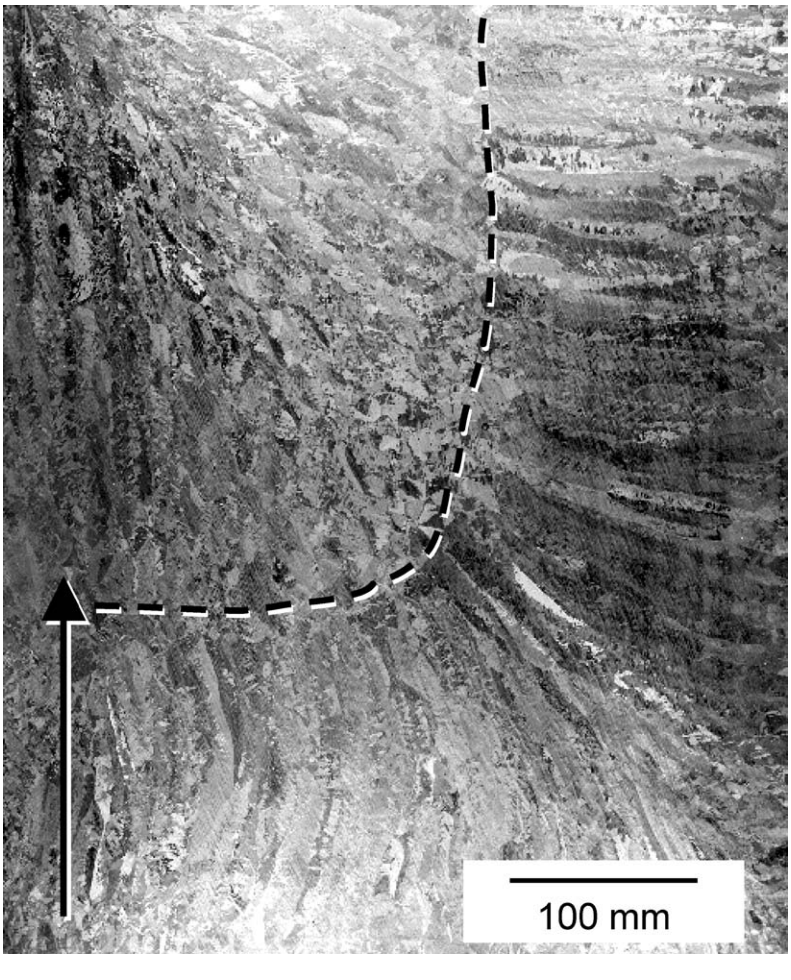


*Figure 1* Polished section of the VAR ingot section, solidified with the stirring field active. The columnar/equiaxed transition boundary is indicated with a dashed line. The arrow shows the growth direction.

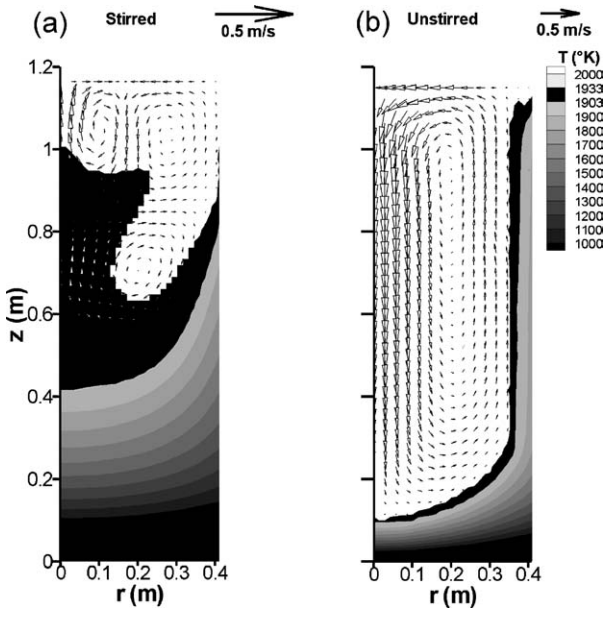


*Figure 2* Macromodel results showing the temperature contours and fluid flow vectors for: (a) stirred and (b) unstirred VAR of Ti6Al4V at 11,756 s into the process. The range of temperature between the liquidus and solidus is rendered black to highlight the extent of the mushy zone. Note the difference in the velocity scale.

nuclei were inserted at the external boundary of the domain, representing the chill zone next to the water-cooled copper jacket. A summary of the parameters and properties used is given in Table I.

## 3. Results and discussion

### 3.1. Experiment

The etched microstructure of the ingot section is shown in Fig. 1. The columnar zone extends to approximately 150 mm from the side edge of the ingot, and approximately 150 mm from the bottom.

### 3.2. Stirring

The macromodel results alone show that the application of the stirring field has a significant effect upon the temperature during the process, due to the change in the liquid flow patterns. Fig. 2 compares the temperature and flow patterns for the same time in the stirred and unstirred cases. The flow cells are quite different; in the stirred case the flow cell is broken into three zones, whereas in the unstirred case there is a single large EMF flow cell. This carries heat down into the ingot resulting in a much narrower mushy zone (rendered in black), leaving a larger area of high temperature and low gradient in the central liquid area. This in turn affects the growth rate and alters the balance between nucleation and growth, changing the boundary between the equiaxed and columnar zones. Fig. 3 shows the mesomodel results for stirred and unstirred cases, using the same nucleation functions; the extent of the columnar zone at the sides is smaller for the stirred case in proportion to the extent at the bottom, compared with the experimental ingot. For the unstirred case, the predicted columnar zone is smaller than is experimentally observed.

The extent of the columnar zone depends on two main factors; the thermal gradient and the rate of advance of the liquidus. Fig. 2 shows a much broader mushy zone with lower temperature gradient in the stirred case than in the unstirred case (at the process time 11,756 s) and at this time the mushy zone (black contour) is much broader in the stirred case. In the unstirred case, the height of the solid formed is much smaller than in the unstirred case; the solidification

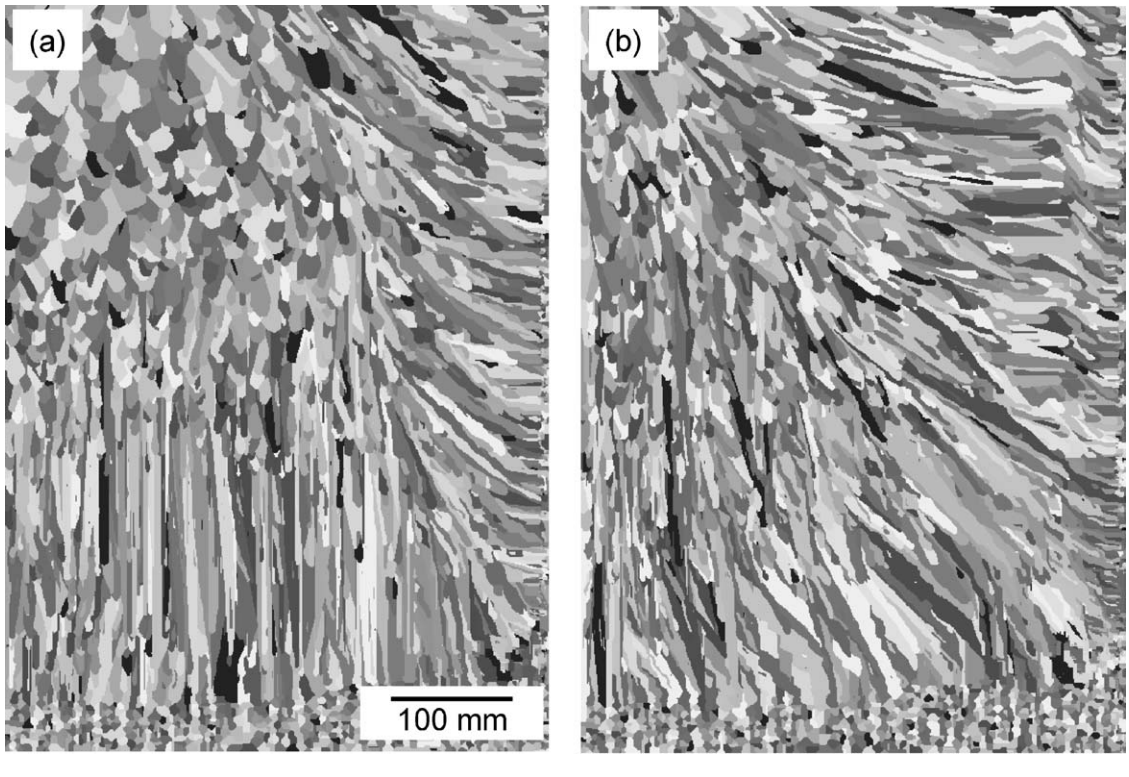


*Figure 3* Mesomodel results showing the predicted microstructure resulting from the macromodels shown in Fig. 2: (a) stirred and (b) unstirred.

front has remained approximately stationary for a much longer part of the process thus inhibiting columnar grain growth. In the stirred case, the growth from the base is faster and more uniform. The higher and more uniform growth of the stirred case favours columnar grain formation at the bottom of the ingot, and the lower gradient developed subsequently favours equiaxed nucleation in the centre of the ingot. However, this is dependent upon the nucleation parameters chosen, as described below.

### 3.3. Nucleation

The columnar to equiaxed transition observed in the experiments and in the simulations, Figs 1 and 3, is not only sensitive to the temperature field but to the nucleation behaviour. If the number density of nuclei is decreased, for example, the columnar grains may grow farther into the ingot. Likewise, if the spread of the distribution of the critical undercooling values is decreased, the columnar grains may persist for longer. However, this variability is limited by the imposed temperature field. If the nucleation is enhanced greatly then the entire simulation becomes equiaxed, likewise if it is suppressed then the entire simulation is columnar. A range of simulations studying the sensitivity of these parameters was run, using the input parameters in Table II.

Fig. 4a shows the visually estimated location of the CET for stirred simulations in which a transition occurred; the distance from the base varies within a range of 200–300 mm, generally lying farther above the base

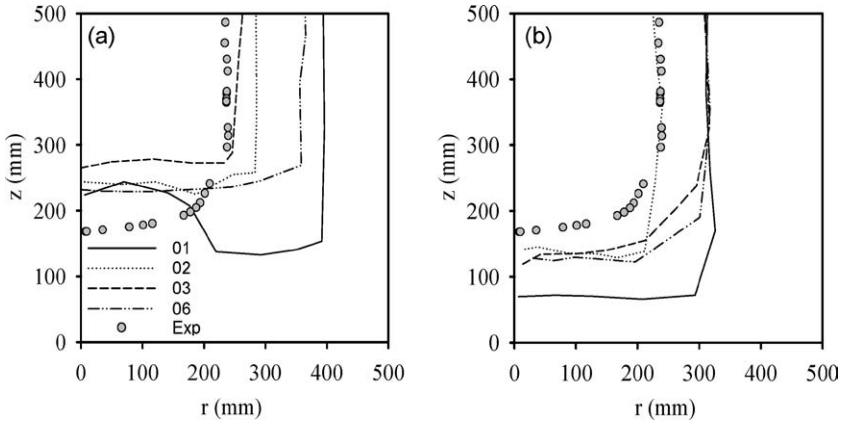


*Figure 4* The effects of nucleation on the columnar-equiaxed transition, compared with the CET for the stirred ingot: (a) stirred and (b) unstirred.

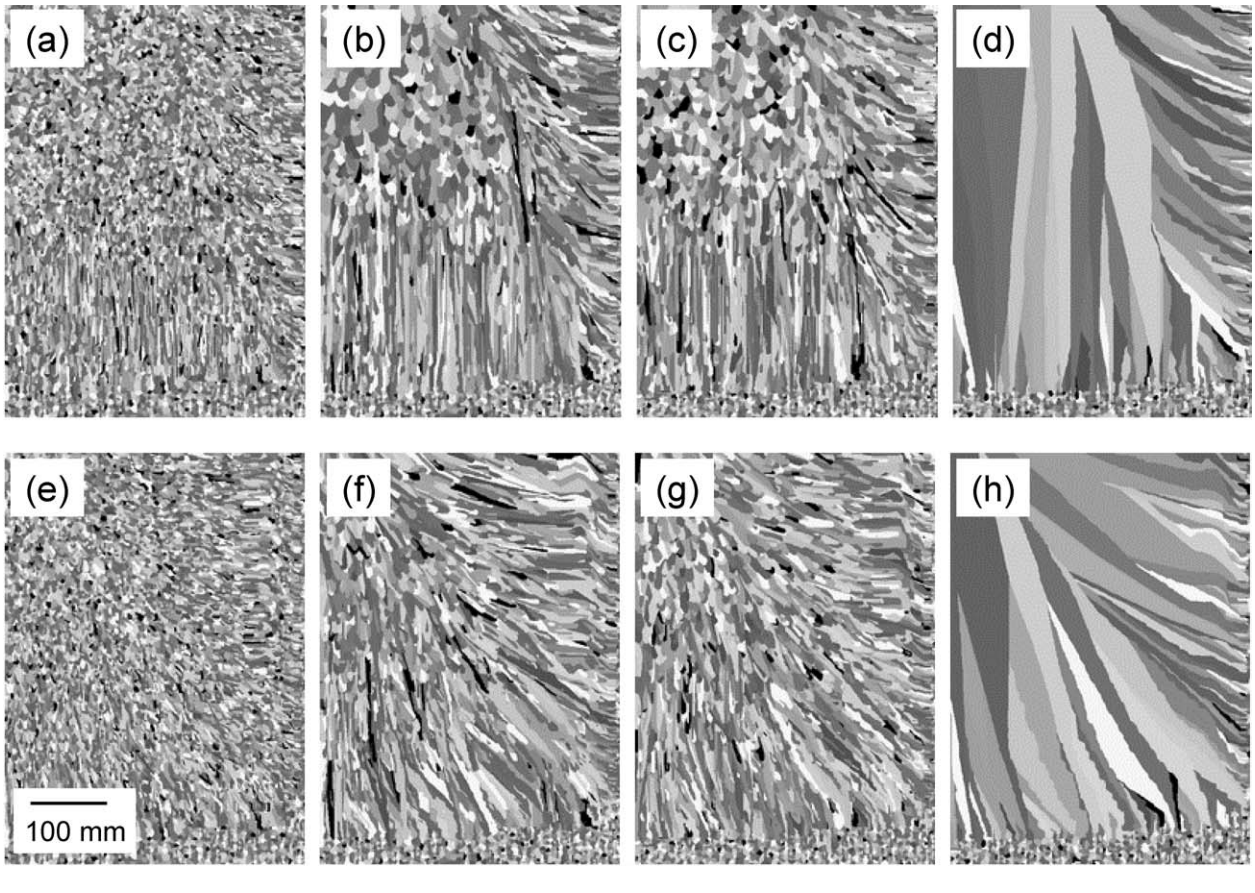


*Figure 5* The effects of nucleation on the columnar-equiaxed transition, illustrated for selected stirred (a–d) and unstirred (e–h) simulations: (a, e) parameter set 01, (b, f) parameter set 02, (c, g) parameter set 03, and (d, h) parameter set 04.

TABLE II Nucleation parameters varied in the simulations

| Parameter set units | $N_n^v$ ($m^{-3}$) | $\Delta T_n$ (K) | $\sigma_n$ (K) |
|---|---|---|---|
| 01 | 5.00E + 07 | 1 | 0.5 |
| 02 | 5.00E + 07 | 4 | 2 |
| 03 | 5.00E + 07 | 1 | 8 |
| 04 | 5.00E + 07 | 32 | 8 |
| 05 | 1.00E + 08 | 1 | 0.5 |
| 06 | 1.00E + 08 | 4 | 2 |
| 07 | 1.00E + 08 | 1 | 8 |
| 08 | 1.00E + 08 | 32 | 8 |
| 09 | 5.00E + 08 | 1 | 0.5 |
| 10 | 5.00E + 08 | 4 | 2 |
| 11 | 5.00E + 08 | 1 | 8 |
| 12 | 5.00E + 08 | 32 | 8 |

than it is in the experimental ingot. Outside the range of parameters giving this transition, the entire ingot is either equiaxed or columnar. At the same time, the transition zone ranges from near zero to 150 mm from the edge of the ingot, always lying closer to the edge than it does in the experimental ingot. Fig. 5 shows a small range of simulations illustrating this behaviour. If the unstirred macromodel is used with the same range of parameters, Fig. 4b, the transition at the edge of the ingot is moved closer to that for the experimental ingot but the transition at the base lies below the experimentally observed location.

The undercooling range that seems to best match the experiments does not likely represent the true nucleation undercooling; the exact effect of the $\Delta T_n$ parameter on the microstructure depends also on the thermophysical parameters and solute transport that affecting the growth rate/undercooling relationship which has not been explored in the present study. Experimental measurements of solute transport properties in liquid titatium would be helpful in improving the model.

The experimental ingot exhibits the long columnar zone at the base typical of the stirred model results, despite the changes in the nucleation parameters. This seems to indicate that neither of the macromodel temperature fields reproduce precisely the true behaviour of the VAR furnace; rather, the real temperature field is somewhere between these two extremes. This may occur due to partial shielding of the magnetic field, as suggested by Bertram *et al.* [1] which progressively increases as more liquid metal enters the mould. Partial shielding would cause the start-up region to more closely resemble the stirred case, whereas regions solidifying at later times would more closely resemble the unstirred case.

### 3.4. Conclusions

A multiscale model of the development of the microstructure during vacuum arc remelting has been implemented by combining a macroscale model for heat, electromagentic effects, and fluid flow with a mesoscale model for nucleation and growth. The model predicted grain structures were compared to those measured in industrial scale ingots with and without electromagnetic stirring. The model predicted the correct trends in the change in location of the columnar to equiaxed transition location, but not the exact locations. Therefore, the model provides a useful tool in predicting the influence of processing parameters upon the changes in structure, but not the exact values of grain size.

## Acknowledgements

The authors would like to acknowledge support from the EPSRC under GR/R61666/01. Some results were generated using code developed by the Specialty Metals Processing Consortium.

## References

1. L. A. BERTRAM, R. S. MINISANDRAM and M. G. VOLAS, in 2001 International Symposium on Liquid Metal Processing and Casting, Santa Fe, NM, USA, 23–26 Sept. 2001 (American Vacuum Society, NY, USA, 2001) p. 225.
2. L. A. BERTRAM, F. SPADAFORA, S. KEMPKA and R. MINISANDRAM, Ti-6-4 Flow under Electromagnetic Stirring and Melt Current Lorentz Force in Industrial Scale VAR: Parameter Sensitivity in Simulations, TMS talk in Sympos. Proc. Synth. and Model. for Prod. And Proc. of Ti and its Alloys, K.O. Yu, chair, TMS Annual Meeting, March 11–17, 2000.
3. L. A. BERTRAM, P. R. SCHUNK, S. N. KEMPKA, F. SPADAFORA and R. MINISANDRAM, *JOM-J. Miner. Met. Mater. Soc.* **50** (1998) 18.
4. L. A. BERTRAM, C. ADASCZIK, R. MINISANDRAM, P. SACKINGER, R. WILLIAMSON, D. EVANS and D. WEGMAN, in 1997 International Symposium on Liquid Metal Processing and Casting, Santa Fe, NM, USA, 16–19 Feb. 1997 (American Vacuum Society, NY, USA, 1997) p. 110.
5. C. A. GANDIN and M. RAPPAZ, *Acta Mater.* **45** (1997) 2187.
6. W. WANG, P. D. LEE and M. MCLEAN, *ibid.* **51** (2003) 2971.
7. X. XU, R. C. ATWOOD, S. SRIDHAR, P. D. LEE, M. MCLEAN, B. DRUMMINGS, R. M. WARD and M. H. JACOBS, in Int. Symp. on Liquid Metal Processing Santa Fe, NM, 1999, p. 76.
8. R. C. ATWOOD and P. D. LEE, in Modelling of Casting Welding and Advanced Solidification Processing IX, edited by P. R. Sahm *et al.* (Aachen, Germany, 2000) p. 2.

*Received 17 March*
*and accepted 29 June 2004*